Title	Accelerated carbonation of different size fractions of MSW IBA and the effect on leaching(Main article)
Author(s)	Lin, Wenlin Yvonne; Heng, Kim Soon; Sun, Xiaolong; Wang, Jing-Yuan
Citation	Lin, W. Y., Heng, K. S., Sun, X., & Wang, J.-Y. (2015). Accelerated carbonation of different size fractions of MSW IBA and the effect on leaching. Waste management, 41, 75-84.
Date	2015
URL	http://hdl.handle.net/10220/34458
Rights	© 2015 Elsevier. This is the author created version of a work that has been peer reviewed and accepted for publication by Waste Management, Elsevier. It incorporates referee's comments but changes resulting from the publishing process, such as copyediting, structural formatting, may not be reflected in this document. The published version is available at: [http://dx.doi.org/10.1016/j.wasman.2015.04.003].

Title: Accelerated carbonation of different size fractions of MSW IBA and the effect on leaching

Authors: Wenlin Yvonne Lin[1,2,*], Kim Soon Heng[2], Xiaolong Sun[2], Jing-Yuan Wang[1,2,*]

Affiliations:

Division of Environmental and Water Resources Engineering, School of Civil and Environmental Engineering, Nanyang Technological University, 50 Nanyang Avenue, Singapore 639798, Singapore[1]

Residues and Resource Reclamation Centre, Nanyang Environment and Water Research Institute, Nanyang Technological University, 1 Cleantech Loop, Singapore 637141, Singapore[2]

*Corresponding authors:

Tel.: +65-6790-4100; Fax: +65-6792-7319

Email address: jywang@ntu.edu.sg (Jing-Yuan Wang)

Tel.: +65-6790-4102; Fax: +65-6792-7319

Email address: wylin1@e.ntu.edu.sg (Wenlin Yvonne Lin)

Contact author:

Wenlin Yvonne Lin

Abstract

Accelerated carbonation has been studied as a treatment method for MSW IBA, and the main advantage is that it can shorten the treatment duration from months to days, compared to natural weathering. This study investigated the effect of accelerated carbonation on different size fractions of IBA collected from two incineration plants in Singapore. The different size fractions were ground to <425 μm to minimise the influence of morphological difference on carbonation efficiency from that of chemical and mineralogical differences. Total element content was carried out for IBA collected from both incineration plants and the different size fractions. XRD was also used to analyse the mineralogical composition of IBA. Results showed that the degree of carbonation decreased as the size increased, which in turn corresponded to decreasing total Ca content and portlandite phase. The leaching behaviour of Pb, Zn, Cu, Cr and soluble constituents like DOC, Cl^-, and SO_4^{2-} were evaluated. It was found that carbonation resulted in the reduction of leaching of most constituents, except Cl^- and SO_4^{2-}. The reduction in leaching after carbonation can be attributed to the decrease in pH and formation of secondary minerals, rather than the precipitation of calcite. The research also suggested that since the leaching of soluble constituents from untreated IBA is mainly from the fine fractions and the fine fractions are more reactive to accelerated carbonation, size separation is beneficial in improving the carbonation efficiency and reducing the volume of IBA that needs to be treated, which can potentially reduce the treatment cost of IBA.

Keywords: Municipal solid waste; Incineration bottom ash; Accelerated carbonation; Leaching; Heavy metal

1. Introduction

With the increase in population and affluence over the past decades, the amount of municipal solid waste (MSW) generated has increased rapidly across the world. This has pressed many countries to implement efficient waste disposal technologies such as incineration to tackle the potential environmental impacts that may arise from improper handling of MSW. Incineration is usually favoured in land-scarce countries such as Japan and Singapore as it is able to reduce the total volume of MSW by up to 90%, thus reducing the amount of land space needed for waste disposal. However, incineration generates incineration bottom ash (IBA) and fly ash (IFA) as end products, which still need proper treatment before disposal in landfill.

Many studies have found that IBA can be recycled as useful materials in the construction industry, as IBA exhibits similar properties to concrete aggregate (Tay and Cheong, 1991; Tay and Goh, 1991; Pera et al., 1997; Filipponi et al., 2003; Müller and Rübner, 2006; Van Dr Wegen et al., 2013). However, while some of the researches focused on deriving the optimum formulation (i.e. the ratio of IBA to cement) for higher compressive strength and to improve other physical properties (e.g. Tay and Cheong, 1991; Tay and Goh, 1991; Filipponi et al., 2003), some pretreatment on IBA is needed to ensure the integrity of the construction material made with IBA. Sieving of IBA is a mandatory pretreatment step in some countries such as Denmark and the Netherlands, which utilise IBA massively (Chandler et al., 1997). The need to sieve IBA arises from the engineering requirement when utilising IBA in aforementioned applications. Firstly, from the engineering viewpoint, the total percentage of fine size fraction (<60 μm) in IBA for use as asphalt pavement (Toraldo et al., 2013) or fill for embankment (Muhunthan et al., 2004) has to be less than 10% as the fine size fraction has high absorption for water, which compromises the durability due to freeze-thaw susceptibility (Chandler et al., 1997).

Furthermore, sieving of IBA is essential for the removal of oversized fraction (i.e. >50 mm) and metallic materials. Non-ferrous metals in IBA, such as Al, are detrimental to the structural integrity due to the evolution of H_2 when IBA comes into contact with water, which results in concrete expansion (Müller and Rübner, 2006; Van Dr Wegen et al., 2013). Lastly, the leachability of certain elements was found to decrease as the size increased (Stegemann and Schneider, 1991). Thus, sieving IBA into different size fractions will help to reduce the treatment cost by reducing the volume of IBA that needs to be treated.

Leaching of trace elements from IBA is another concern that deters the utilisation of IBA. Before IBA can be utilised, it must first comply with the environmental regulations that are presiding in the country. One of the most commonly studied treatment methods is accelerated carbonation. This technology is derived primarily from natural weathering or aging process, where CO_2 reacts with abundantly available alkaline rocks in the natural environment (Lackner et al., 1995). This thermodynamically favoured process converts the CO_2 gas to form stable carbonate mineral forms. IBA contains high amounts of alkaline metal oxides, which are capable of performing the same process as alkaline rocks (Costa et al., 2007). This process causes the pH of the IBA to decrease and calcite to precipitate until the material is in equilibrium with atmospheric CO_2 (Meima and Comans, 1999). These changes have been found to influence the leaching behaviour of IBA. Generally, most literature found that the leaching of Pb, Zn and Cu reduces significantly within a short period during accelerated carbonation treatment (Fernández Bertos et al., 2004; Arickx et al., 2006).

The main advantage of using accelerated carbonation to treat IBA, compared to natural weathering, is the reduction in the leaching of certain trace elements in a shorter time (from months to days). Various parameters, such as moisture content, temperature and CO_2 percentage,

92 that affect the efficiency of accelerated carbonation has been identified and studied (Arickx et al.,
93 2006; Costa et al., 2007; Nam et al., 2012). With the establishment of the optimum range of
94 various parameters (Costa et al., 2007), the focus of studying accelerated carbonation has shifted
95 to improve the understanding on the leaching mechanism due to the effect of accelerated
96 carbonation. Meima and Comans (1999) suggested that the reduction in Pb and Zn leaching was
97 due to the drop in pH after IBA carbonated. The formation of secondary minerals after
98 carbonation, such as Fe/Al (hydr)oxides, has been proposed to reduce leaching through sorption
99 (Cornelis et al., 2008; Arickx et al., 2010).

100 It is challenging to identify the causes for all the changes of IBA leaching behaviour after
101 accelerated carbonation, especially when the influencing factors are interacting. This study
102 focuses on the chemistry of accelerated carbonation with IBA through investigating the
103 mineralogy of different size fractions and therefore, understands its effect on leaching. Thus far,
104 there were not many studies on the response of different size fractions towards accelerated
105 carbonation (Chimenos et al., 2003; Baciocchi et al., 2010). Chimenos et al. (2003) studied the
106 effect of natural weathering on different size fractions of MSW IBA while Baciocchi et al.
107 (2010) applied accelerated carbonation on IBA from refuse derived fuel incinerator. On the other
108 hand, this study investigates the effect of accelerated carbonation treatment on the different size
109 fractions of MSW IBA. Consequently, this study explores the use of sieving before the
110 accelerated carbonation treatment and its effect on the leaching behavior of each size fraction.

111 **2. Materials and methods**

112 2.1 Sampling and handling of IBA

113 The IBA used for this study was collected from two incineration plants in Singapore.
114 Incineration plant S receives predominantly domestic waste (approximately 60%) while

incineration plant T receives predominantly industrial waste (approximately 60%), in addition to household waste. The IBA samples were collected before metal separation by the magnetic separator inside the incineration plants. The wet IBA was a mixture of grate sifting, boiler and economizer ash, and grate ash combined at the quenching tank. Approximately 50 kg of wet, freshly quenched IBA was collected separately from each plant. The wet IBA was immediately dried at 40°C for 3 days upon collection. A portion of the dried IBA was tested for loss of ignition (LOI). The rest of the dried IBA was sieved to obtain four size fractions: 0-2 mm (S0-2 and T0-2), 2-4 mm (S2-4 and T2-4), 4-20 mm (S4-20 and T4-20) and 20-50 mm (S20-50 and T20-50). The weight of the oversized fraction, i.e. >50 mm, was recorded but was not used in the carbonation study. The ferrous and non-ferrous metals which could not be crushed were removed and weighed. All the size fractions were further ground using a ball mill to <425 μm. Although in an actual industrial application, it is not economically practical to reduce the particle size of coarse IBA by grinding, the purpose of doing this is to minimise the influence of morphological difference between different size fractions on carbonation efficiency. This also ensures that the effect on carbonation will mainly come from the chemical and mineralogical differences between different samples.

2.2 Characterisation

Total element content of each size fraction was determined by digestion with aqua regia followed by HF, and the solution was analyzed for cations using Inductively Coupled Plasma – Mass Spectrometer (ICP-MS Nexlon 300D, Perkin Elmer) and anions using Ion Chromatography (IC 882 Compact IC Plus, Metrohm). The true densities of the four size fractions of the untreated samples were determined by automatic density analyzer (Ultrapyc 1200e).

2.3 X-ray diffraction (XRD)

XRD analysis was performed on untreated IBA samples. Before analysis, the samples were further ground using a mortar and pestle. XRD analysis was then performed in Bragg-Brentano geometry (Bruker AXS D8 Advance) with Cu-Kα radiation (λ = 1.54060Å) and fixed receiving slit (2.0 mm). The scan speed was set at 0.3°/min, with a scan step of 0.02° in continuous scan mode. Mineral identification was done by comparing the positions of the measured diffraction maxima with peak positions of possible minerals contained in the ICDD powder diffraction file database (ICDD, 2001).

2.4 Accelerated carbonation

The accelerated carbonation process was carried out in CO_2 incubator (Sanyo MCO-18AIC), using 20% CO_2 at 1 atm for all the experiments. A tray of deionised (DI) water was placed at the bottom of the incubator to maintain a constant atmospheric humidity. A preliminary study was carried out to determine the optimum operating conditions using 0-2 mm size fractions only, using the same set up as mentioned here. In the preliminary study, the accelerated carbonation was carried out for a week. It was observed that 2 hours of carbonation was sufficient to reach a saturation point, after which the reaction rate decreased significantly. The optimum operating conditions that led to the highest degree of carbonation observed at 2 hours of carbonation was applied to the other size fractions in this study: 35°C and 50°C at 15% moisture content. The required moisture content was obtained by adding DI water to dried and ground IBA. IBA was spread on plastic petri dishes to no more than 2 mm thick and at approximately the same dry mass. The carbonation was stopped after 2 hours. The actual moisture of IBA remaining in the petri dish was monitored.

2.5 Degree of carbonation

160 The degree of carbonation was evaluated by measuring the amount of carbonate content
161 formed after subjected to accelerated carbonation. The amount of carbonate content was
162 measured using Analytik Jena Multi N/C 2100/2100S (solid module), which measures the
163 concentration of CO_2 released from IBA at 900°C using non-dispersive infrared sensor. The
164 degree of carbonation (mg/g) was calculated by subtracting the initial carbonate value of the
165 respective untreated samples from the carbonate content present in IBA samples after 2 hours of
166 carbonation. Triplicate analysis was done.

167 2.6 Leaching

168 The change in leaching behaviour of IBA after carbonation was evaluated using EN
169 12457-2. Triplicate leaching tests were done. To determine the acid neutralisation capacity
170 (ANC) of the four size fractions of IBA, pH dependence leaching test based on CEN/TS 14429
171 was carried on the untreated samples. The leachates were filtered through 0.45 µm nylon
172 membrane. The pH was measured by Mettler-Toledo G20 Compact Titrator. A portion of the
173 leachate was analysed for anions (Cl^- and SO_4^{2-}) by Dionex ICS-1100 RFIC Ion Chromatography
174 (IC) System and dissolved organic content (DOC) content by Analytik Jena Multi N/C
175 2100/2100S (liquid module). Another portion of the leachate was acidified to pH 2 and analysed
176 for cations by Inductively Coupled Plasma – Optical Emission Spectrometer (ICP-OES from
177 Perkin Elmer Optima 8300).

178 3. **Results and discussion**

179 3.1 Characteristics of IBA

180 Table 1 shows the physical characteristics of IBA collected from the two incineration
181 plants. The oversize fraction of >50 mm was not used in this study but their weight percentages
182 were noted as 4 wt% and 13 wt% from S and T respectively. Both plants showed higher weight

183 percentages for 0-2 mm and 4-20 mm size fractions than other fractions. The true density was
184 found to increase as the size increased for T samples but not for S. The density for the different
185 size fractions of S samples was quite close to one another. The high moisture content (16.8% for
186 S and 15.5% for T) was due to the sampling of IBA near to the exit of the quenching tank for
187 both incineration plants. The LOI values for both plants (0.59% for S and 1.51% for T) were
188 found to be much lower than mean values reported in Canada (2.65-29.2%), Denmark (1.9-6.3%)
189 and United States (3.7-6.4%) (Chandler et al., 1997).

190 The total element content for the four size fractions is shown in Table 2. Only the total
191 contents of Ca, Cd, Co, Sb, Cl^- and SO_4^{2-} were observed to decrease as the size increased for
192 both incineration plants. For the soluble salts, i.e. Cl^- and SO_4^{2-}, this trend shows that sieving can
193 be beneficial to IBA utilisation in concrete by selecting only coarser size fractions, in which the
194 soluble salts contents are lower. This will minimise expansion problems arising from reactions
195 associated with soluble salts (Tyrer, 2013). However, the 20-50 mm size fraction has the highest
196 total Al content among all the size fractions, which will be unfavourable in IBA utilisation in
197 concrete due to Al-induced expansion. However, this can be resolved by immersing IBA in
198 NaOH, which reacts with Al to emit H_2 before utilisation (Pera et al., 1997). Other elements such
199 as Cr was found to decrease in S sample as the size increased but increase in T sample as the size
200 increased. For Cu, it was found to be most concentrated in S2-4 and T0-2. For Mn and Pb, both
201 were highest in 2-4 mm size fraction while Zn was mostly concentrated in 0-2 mm. The trend of
202 total element content of Ca, Pb and Zn as a function of the size fraction was similar to those
203 reported by Chimenos et al. (2003).

204 Comparing between the two incineration plants, Pb, Sb, Sn and Cl^- were present in higher
205 concentrations in all the size fractions of S than T sample. The major sources of Sb include flame

206 retardants and batteries. Pb is also a major component in batteries. Sn is used in the coating of
207 steel cans and Cl^- can be found in PVC plastics and food waste. All these are common household
208 wastes, which are not compulsory to be segregated for recycling in Singapore and hence, this
209 could explain the higher concentrations of Pb, Sb, Sn and Cl^- in S sample since incineration plant
210 S receives predominantly household waste. On the other hand, Fe, Mn and Mo were found to be
211 at higher concentration in all the size fractions of T sample. Mn and Mo are mainly used as alloy
212 in metallurgy while Fe is used for the production of ferrous materials. These elements mainly
213 come from industrial wastes, which incineration plant T receives predominantly. These
214 metallurgy wastes could have contributed to the higher true density for the coarser size fraction
215 in T samples.

216 Figure 1 shows the XRD patterns of untreated IBA samples of 0-2 mm size fraction. The
217 mineralogical compositions from different incineration plants were found to be slightly different.
218 Diopside ($CaMg(Si_2O_6)$) was undetectable in S0-2 sample while hydroxylapatite ($Ca_5(PO_4)_3(OH)$)
219 and gibbsite ($Al(OH)_3$) were undetectable in T0-2 sample. The dominant anhydrite ($CaSO_4$) peak
220 was also significantly higher than the quartz (SiO_2) peak in S0-2, in contrast to T0-2. Both
221 hematite (Fe_2O_3) and magnetite (Fe_3O_4) peaks were detected in S0-2 and T0-2 but they were
222 labeled in T0-2 only as the intensity of the peaks was more observable. The differences in
223 mineralogical composition and in the total element content between the IBA of the two
224 incineration plants contribute to the different optimum carbonation temperature for S and T
225 samples.

226 XRD analysis was also carried out for the different size fractions of untreated T samples to
227 determine the difference in mineralogical compositions (Figure 2). Generally, all the size
228 fractions have similar mineralogical composition but with different characteristic peak intensity

for each phase. Anhydrite, hematite, portlandite ($Ca(OH)_2$) and calcite ($CaCO_3$) peaks showed decreasing intensity as the size of T samples increased. On the other hand, magnetite peaks increased with the size of T samples. Anhydrite and diopside minerals are formed during the quenching process while calcite is present as a remnant from the combustion process (Speiser et al., 2000). Overall, the XRD patterns showed the untreated IBA samples have high crystallinity, although IBA is commonly known to have high content of amorphous phase. This could be due to the inclusion of grate sifting, boiler and economiser ash to the IBA in this study.

3.2 Degree of carbonation of different size fractions

Based on our preliminary study, the optimum operating conditions were 2 hours of carbonation at 15% moisture content for both S and T samples. Fernández Bertos et al. (2004) reported 75% of carbonation reaction took place in the first 2.5 hours, whereas another study done by Baciocchi et al. (2010) reported significant increase in carbonate at 8 hours of carbonation. In comparison, 2 hours of carbonation in our study was relatively fast and this could be due to the presence of grate sifting, boiler and economiser ash in the IBA. The carbonated temperatures for S0-2 and T0-2 samples were 35°C and 50°C respectively. Both 35°C and 50°C were used for carbonating the four size fractions of S and T samples for comparison on the difference in degree of carbonation (Table 3). Generally, the degree of carbonation for the four size fractions decreased as the size increased. This decrease in the degree of carbonation corresponded to the decrease in the total Ca content and portlandite phase as the size increased. This result echoed the findings of Baciocchi et al. (2010) and demonstrated that the amount of CO_2 sequestrated by IBA is strongly dependent on the total Ca content.

In terms of the optimum operating conditions, S samples carbonated more effectively at 35°C, 15% moisture content, except for S20-50 sample. The same trend was observed for T

252 samples for operating conditions of 50°C, 15% moisture content, except for T4-20 sample.
253 However, the differences in the degree of carbonation for the exceptions were not great. In fact,
254 there was very minute difference in degree of carbonation for 4-20 mm and 20-50 mm size
255 fractions. This suggests that the coarse size fractions were not as sensitive to the selected
256 operating conditions as fine fractions.

257 Lastly, the actual moisture content remaining after 2 hours of carbonation was observed to
258 be similar with respect to the carbonated temperatures, regardless of the source of IBA. The
259 actual moisture content of all the size fractions from both plants had an average value of 14.3%
260 at 35°C, while the average value at 50°C was 10.6%. This shows that the temperature used for
261 carbonation would result in some loss of moisture with time.

262 3.3 Effect of accelerated carbonation on pH

263 Figure 3 shows the pH before and after carbonation at 35°C and 50°C, 15% moisture
264 content. For the untreated S samples, the pH did not vary much among the four size fractions,
265 from pH 12.4 to 12.1 (i.e. from finest to coarsest). However, the pH was found to decrease
266 slightly from pH 12.6 to 11.9 as the size increased for the untreated T samples. After 2 hours of
267 carbonation, all studied samples' pH dropped to below 10, and the lowest observed pH was 8.9
268 for S4-20 sample carbonated at 35°C and 15% moisture content.

269 3.4 Effect of accelerated carbonation on leaching

270 Figure 4 shows the XRD patterns of T0-2 and T20-50 samples before and after carbonation
271 at 50°C and 15% moisture content. The calcite peaks for both T0-2 and T20-50 samples
272 increased after carbonation, together with the disappearance of portlandite peaks, which explains
273 the decrease in pH after carbonation due to the conversion of portlandite to calcite.

The decrease in pH after carbonation for all the size fractions has a positive impact on the reduction in Pb and Zn leaching, whereby the leaching mechanism of Pb and Zn is reported to be dependent on the pH of IBA (Meima and Comans, 1999). The leaching trend for Pb was not shown here as most of the IBA leachates were below the detection limit of ICP-OES (i.e. <5 µg/L). Untreated S0-2 and S2-4 had the highest Pb released at 30.0 mg/kg and 73.1 mg/kg respectively while Pb released for untreated S4-20 was 1.0 mg/kg. The inclusion of grate sifting, boiler and economiser ash to the IBA in this study could have resulted in the relatively higher Pb leaching from untreated samples. Untreated T0-2 was found to leach slightly at 0.36 mg/kg. The rest of the untreated size fractions in both S and T samples were undetectable in Pb leaching. However, accelerated carbonation was found to be very effective in reducing Pb leaching. Regardless of the size fractions and operating conditions of carbonation, Pb was undetectable after carbonation. This consistency in reduction of Pb leaching suggests that pH plays a dominant role in the leaching mechanism of Pb. For Zn, the amount of Zn released from untreated S and T samples decreased as the size increased (Figure 5 (a, b)). Generally, all the size fractions from untreated T sample showed significantly less Zn leaching compared to those from untreated S sample. This leaching trend showed no relation to the total Zn content of S and T samples. After carbonation, only S0-2 and T0-2 samples still had slight Zn leaching while the rest of the size fractions were below the detection limit of ICP-OES (i.e. <5 µg/L).

Similarly, Cu leaching decreased as the size increased for the untreated samples (Figure 5 (c, d)). However, unlike Pb and Zn, the percentage reduction varied for Cu after carbonation. The percentage reduction in Cu leaching ranged from 64.8% to 85.3% for S samples and 69.5 to 82.4% for T samples. Since the pH after carbonation for all the samples was consistently around 9, this suggests that the leaching mechanism of Cu was not strongly influenced by pH, but by

297 other factors. In terms of the degree of carbonation, the reduction in Cu leaching was observed to
298 be unaffected by the difference in carbonated temperatures. Figure 6 shows the correlation
299 between the amount of Cu and DOC released was high, even at different carbonation
300 temperatures. This suggests that Cu leaching is greatly influenced by DOC leaching due to the
301 formation of more soluble organic complexes, instead of the degree of carbonation. Arickx et al.
302 (2010) proposed that the sorption of fulvic acid to secondary minerals like Fe/Al (hydr)oxides
303 formed after carbonation indirectly resulted in the reduction of Cu leaching.

304 In contrast, the amount of Cr released from untreated T samples decreased as the size
305 increased, but S samples did not show the same trend as Cr leaching from untreated S2-4 sample
306 was exceptionally low (Figure 5 (e, f)). This observation corresponded inversely to the total Cr
307 content for S and T samples. After carbonation, S0-2 sample had an average of 48.3% reduction
308 in Cr leaching while the other size fractions of S samples had more significant reduction in Cr
309 leaching, ranging from 63.1 to 92.9%. Similarly, the reduction in Cr leaching for T0-2 samples
310 was an average of 62.2%, which was less significant compared to other size fractions (i.e. 83.0-
311 94.9%). Cornelis et al. (2008) suggested Fe oxides as possible adsorption site for oxyanions,
312 such as Cr. The increasing magnetite content in coarser T samples could have contributed to
313 more significant reduction in Cr leaching (Figure 2). Moreover, the magnetite peaks in T20-50
314 showed observable increase in intensity after carbonation, compared to T0-2, which further
315 supports the possibility that greater Cr reduction in coarser T samples was due to magnetite
316 formation after carbonation.

317 Figure 7 shows the leaching trend of the soluble constituents (i.e. DOC, Cl^- and SO_4^{2-})
318 from the different size fractions of IBA. The leaching of the soluble constituents from untreated
319 IBA showed consistent decrement in concentrations as the size increased. After carbonation,

DOC leaching decreased but did not differ much between the two carbonated temperatures of the same size fractions of the same source of IBA. Similar to Cu, the degree of carbonation did not have much effect on DOC reduction. The percentage reduction for DOC ranges from 11.0% to 32.3% for all the size fractions and source of IBA, whereby S4-20 and T4-20 had the highest reduction. Again, this greater reduction in coarse size fraction could be due to the sorption to Fe oxide formed after carbonation as proposed by Arickx et al. (2010).

For Cl^-, it did not show reduction in leaching after carbonation, while SO_4^{2-} leaching increased after carbonation. The increase in SO_4^{2-} leaching could be due to the conversion of anhydrite to calcite, as can be seen from the decreasing anhydrite peaks in Figure 4(a). However, the anhydrite peaks in T20-50 showed slight increase after carbonation (Figure 4(b)), which did not lead to decrease in SO_4^{2-} leaching for T20-50 samples. Fernández Bertos et al. (2004) also reported an increase in gypsum ($CaSO_4.2H_2O$) after carbonation. Other mineral, such as ettringite, is known to contribute to SO_4^{2-} leaching (Meima et al., 2002) due to its dissolution after carbonation. However, ettringite was not detectable in this study.

3.5 Effect of different size fractions on ANC

The ANC of the different size fractions was investigated (Figure 8). The ANC for both S and T samples was observed to decrease as the size increased. However, the ANC of 0-2 mm size fractions for both S and T samples was significantly higher than the rest of the size fractions. Both S0-2 and T0-2 samples required approximately 1.33 mol H^+/kg of acid to reduce the pH from the initial of around 12 to 10. This amount of acid required was about 2 to 3 times higher than those required by other size fractions to reach a pH of 10. In fact, at around pH 10, the pH of other size fractions were found to decrease significantly from pH 10 to 7 with just an addition of 0.5 to 1 mol H^+/kg of acid. The decreasing ANC as size increased was associated with the

lower buffer capacity due to decreasing portlandite phase, whereby portlandite was reported to be a major contributor to the buffering capacity of IBA (You et al., 2006). The implication of this result in terms of carbonation means that 0-2 mm size fraction requires more CO_2 uptake (i.e. higher CO_2 percentage or longer carbonation duration) to reduce the pH from alkaline to neutral and the other size fractions require less.

4. Conclusions

This study evaluated the effect of accelerated carbonation on different size fractions of IBA collected from two incineration plants in Singapore. Before analysis, the different size fractions were ground to <425 μm. By doing so, the influence of morphological difference between different size fractions on carbonation efficiency can be minimised, and the consequent effect on metal leaching comes mainly from the chemical and mineralogical differences between different IBA samples. The differences between the IBA collected from different incineration plants and their different size fractions were examined through total element content and XRD. The total element content between the two incineration plants showed significant differences for certain elements (i.e. Pb, Sb, Sn, Cl^-, Fe, Mn and Mo), which could be associated with the dominant type of waste received by the plants. In addition, the differences in mineralogical composition of IBA from the two incineration plants contributed to the different optimum temperature for carbonation. In terms of different size fractions, the total element content showed that only some of the elements (i.e. Ca, Cd, Co, Sb, Cl^- and SO_4^{2-}) displayed decreasing total content as the size increased. This trend is especially important for total Ca content as the decreasing Ca content with increased size resulted in decreasing degree of carbonation. However, the 4-20 mm and 20-50 mm size fractions from both sources of IBA did not show significant difference in degree of carbonation when different carbonated temperatures were

366 used. The peaks of certain minerals like anhydrite, hematite, portlandite and calcite also showed
367 decreasing intensity with increased size. This phenomenon was found to influence the percentage
368 reduction of the leaching of Cr and DOC.

369 In general, the pH of IBA reduced from around 12 to 9 after accelerated carbonation. Pb,
370 Zn, Cu, Cr and DOC leaching decreased after carbonation, while carbonation did not affect Cl^-
371 leaching. SO_4^{2-} leaching increased significantly after carbonation. Generally, the amount of
372 leaching after carbonation did not correspond to the degree of carbonation when compared
373 among the same size fraction and source of IBA. The leaching mechanism of IBA was not
374 sensitive to the different operating conditions used, which in this case was the carbonated
375 temperature. Reduction in Pb and Zn leaching was attributed to pH. In contrast, the varying
376 percentage reduction in Cr and DOC leaching was due to the different mineral content in the
377 different size fractions, as observed from the peak intensity of XRD pattern. Cu leaching could
378 also be affected by the different size fractions as it was found to have high correlation to DOC
379 leaching. It seems that the increase in calcite after carbonation was not the main contributor to
380 the reduction in leaching. Rather, the effect of carbonation resulted in the decrease in pH and the
381 formation of secondary minerals (magnetite as found in this study), which then contributed to the
382 reduction in leaching of the trace elements discussed here. Moreover, due to the difference in
383 mineral content in the different size fractions, the effect of carbonation on the different size
384 fractions resulted in varying degree of percentage reduction in leaching.

385 In terms of size effect, most of the elements showed decrease in leaching for the untreated
386 IBA as the size increased. This finding is important especially for highly soluble constituents like
387 DOC, Cl^- and SO_4^{2-}, where the concentration in the 20-50 mm size fraction was significantly
388 lesser compared to 0-2 mm size fraction. Thus size separation can help to increase the utilisation

potential of IBA for the coarse size fraction as the coarse size fraction can generally be used with less treatment, depending on the regulation of each country. Furthermore, ANC results showed that 0-2 mm size fraction required more acid to reduce the pH as compared to other size fractions. Hence, it is possible that the carbonation duration may be further reduced for the coarse size fractions to achieve similar reduction in leaching as discussed in this study. This translates to monetary saving as sieving is simple and inexpensive to carry out.

References

Arickx, S., Van Gerven T., Vandecasteele C., 2006. Accelerated carbonation for treatment of MSWI bottom ash. Journal of Hazardous Materials 137 (1), 235-243.

Arickx, S., De Borger, V., Van Gerven, T., Vandecasteele, C., 2010. Effect of carbonation on the leaching of organic carbon and of copper from MSWI bottom ash. Waste Management 30 (7), 1296-1302.

Baciocchi, R., Costa, G., Lategano, E., Marini, C., Polettini, A., Pomi, R., Postorino, P., Rocca, S., 2010. Accelerated carbonation of different size fractions of bottom ash from RDF incineration. Waste Management 30 (7), 1310-1317.

Chandler, J., Eighmy, T.T., Hartlén, J., Hjelmar, O., Kosson, D.S., Sawell, S.E., Van der Sloot, H., Vehlow J., 1997. Municipal Solid Waste Incinerator Residues. In: Studies in Environmental Science, Vol. 67, Elsevier: Amsterdam, The Netherlands.

412 Chimenos, J. M., Fernández, A. I., Miralles, L., Segarra M., Espiell F., 2003. Short-term natural
413 weathering of MSWI bottom ash as a function of particle size. Waste Management 23 (10), 887-
414 895.
415
416 Cornelis, G., Johnson, C. A., Gerven, T.V., Vandecasteele, C., 2008. Leaching mechanisms of
417 oxyanionic metalloid and metal species in alkaline solid wastes: A review. Applied
418 Geochemistry 23 (5), 955-976.
419
420 Costa, G., Baciocchi, R., Polettini, A., Pomi, R., Hills, C.D., Carey, P.J., 2007. Current status and
421 perspectives of accelerated carbonation processes on municipal waste combustion residues.
422 Environmental Monitoring and Assessment 135 (1-3), 55-75.
423
424 Fernández Bertos, M., Li, X., Simons, S.J.R., Hills, C.D., Carey, P.J., 2004. Investigation of
425 accelerated carbonation for the stabilization of MSW incinerator ashes and the sequestration of
426 CO_2. Green Chemistry 6 (8), 428-436.
427
428 Filipponi, P., Polettini, A., Pomi R., Sirini P., 2003. Physical and mechanical properties of
429 cement-based products containing incineration bottom ash. Waste Management 23 (2), 145-156.
430
431 International Centre for Diffraction Data (ICDD) (2001). The Powder Diffraction File (PDF).
432
433 Lackner, K.S., Wendt, C.H., Butt, D.P., Joyce, E.L., Sharp, D.H., 1995. Carbon dioxide disposal
434 in carbonate minerals. Energy 20 (11), 1153-1170.

435

436 Meima, J. A. and Comans, R. N. J., 1999. The leaching of trace elements from municipal solid
437 waste incinerator bottom ash at different stages of weathering. Applied Geochemistry 14 (2),
438 159-171.

439

440 Meima, J. A., Van Der Weijden, R. D., Eighmy, T. T., Comans, R. N. J., 2002. Carbonation
441 processes in municipal solid waste incinerator bottom ash and their effect on the leaching of
442 copper and molybdenum. Applied Geochemistry 17 (12), 1503-1513.

443

444 Muhunthan, B., Taha, R., Said, J., 2004. Geotechnical engineering properties of incinerator ash
445 mixes. Journal of the Air and Waste Management Association 54 (8), 985-991.

446

447 Müller, U. and Rübner, K., 2006. The microstructure of concrete made with municipal waste
448 incinerator bottom ash as an aggregate component. Cement and Concrete Research 36 (8), 1434-
449 1443.

450

451 Nam, S.-Y., Seo, J., Thriveni, T., Ahn, J.-W., 2012. Accelerated carbonation of municipal solid
452 waste incineration bottom ash for CO_2 sequestration. Geosystem Engineering 15 (4), 305-311.

453

454 Pera, J., Coutaz, L., Ambroise, J., Chababbet, M., 1997. Use of incinerator bottom ash in
455 concrete. Cement and Concrete Research 27 (1), 1-5.

456

457 Speiser, C., Baumann, T., Niessner, R., 2000. Morphological and chemical characterization of
458 calcium-hydrate phases formed in alteration processes of deposited municipal solid waste
459 incinerator bottom ash. Environmental Science and Technology 34 (23), 5030-5037.
460
461 Stegemann, J. A. and Schneider, J., 1991. Leaching potential of municipal waste incinerator
462 bottom ash as a function of particle size distribution. Studies in Environmental Science. Volume
463 48, 135-143.
464
465 Tay, J.H. and Cheong, H.K., 1991. Use of ash derived from refuse incineration as a partial
466 replacement of cement. Cement and Concrete Composites 13 (3), 171-175.
467
468 Tay, J.H. and Goh, A.T.C., 1991. Engineering properties of incinerator residue. Journal of
469 Environmental Engineering 117 (2), 224-235.
470
471 Toraldo, E., Saponaro, S., Careghini, A., Mariani, E., 2013. Use of stabilized bottom ash for
472 bound layers of road pavements. Journal of Environmental Management 121, 117-123.
473
474 Tyrer, M., 2013. Municipal solid waste incinerator (MSWI) concrete. In: Pacheco-Torgal, F.,
475 Jalali, S., Labrincha, J., John, V.M. (Eds.), Eco-efficient concrete. Woodhead Publishing
476 Limited, Cambridge, United Kingdom, pp. 273-310.
477
478 Van Dr Wegen, G., Hofstra, U., Speerstra, J., 2013. Upgraded MSWI bottom ash as aggregate in
479 concrete. Waste and Biomass Valorization 4 (4), 737-743.

480

481 You, G.-S., Ahn, J-W., Han, G.-C., Cho, H.-C., 2006. Neutralizing capacity of bottom ash from

482 municipal solid waste incineration of different particle size. Korean Journal of Chemical

483 Engineering 23 (2), 237-240.

484

FIGURES

Figure 1. XRD patterns of untreated (a) S0-2 and (b) T0-2 samples. [An = anhydrite, Ca = calcite, D = diopside, Gib = gibbsite, H = hematite, Ha = hydroxylapatite, M = magnetite, P = portlandite, Q = quartz]

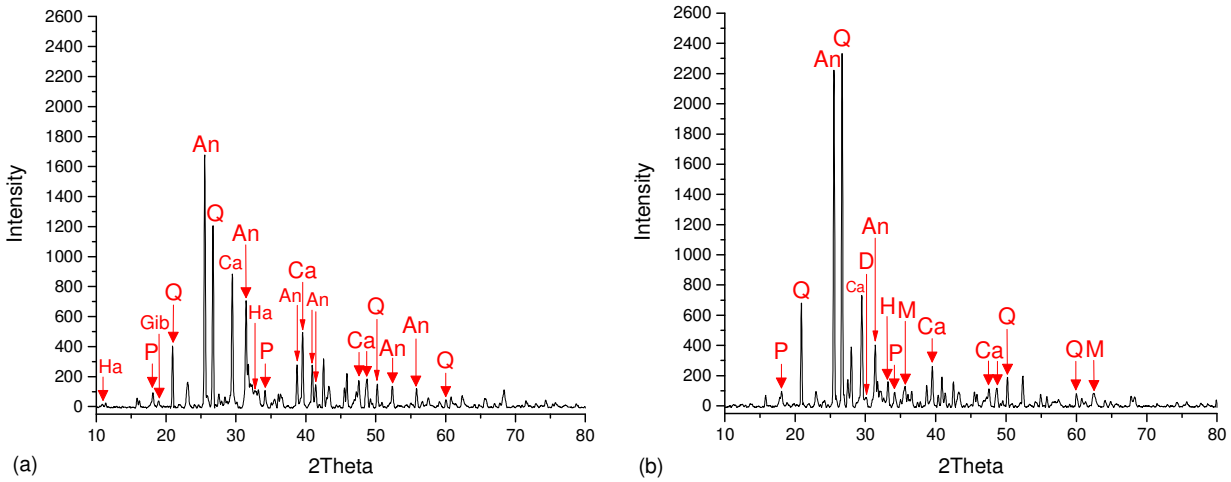

Figure 2. XRD patterns of untreated T0-2, T2-4, T4-20 and T20-50 samples. [An = anhydrite, Ca = calcite, D = diopside, H = hematite, M = magnetite, P = portlandite, Q = quartz]

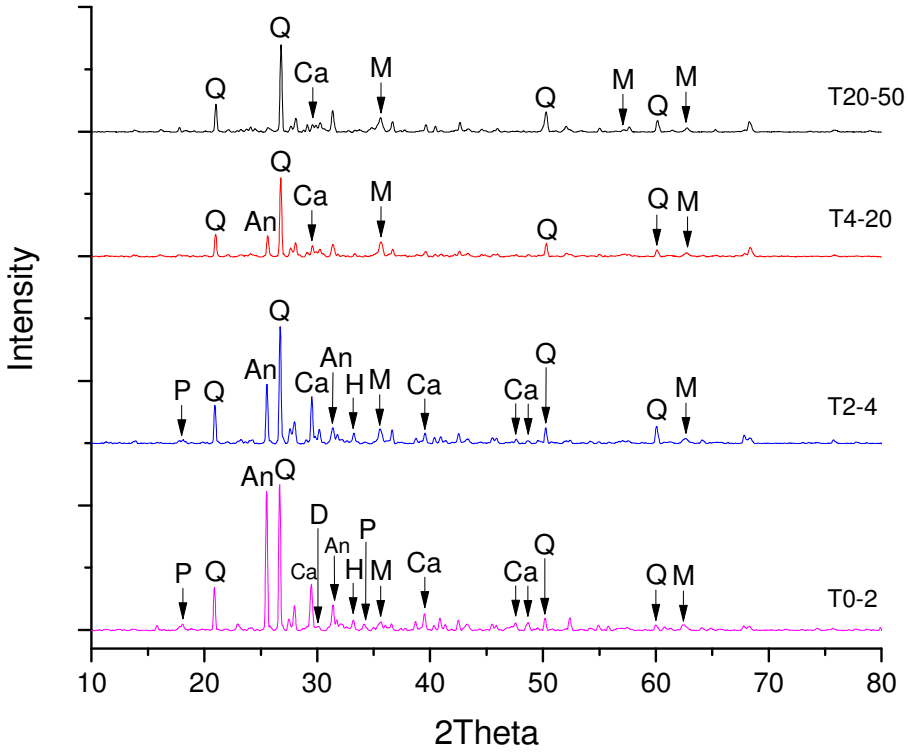

Figure 3. pH of different size fractions showing untreated and carbonated (a) S and (b) T samples.

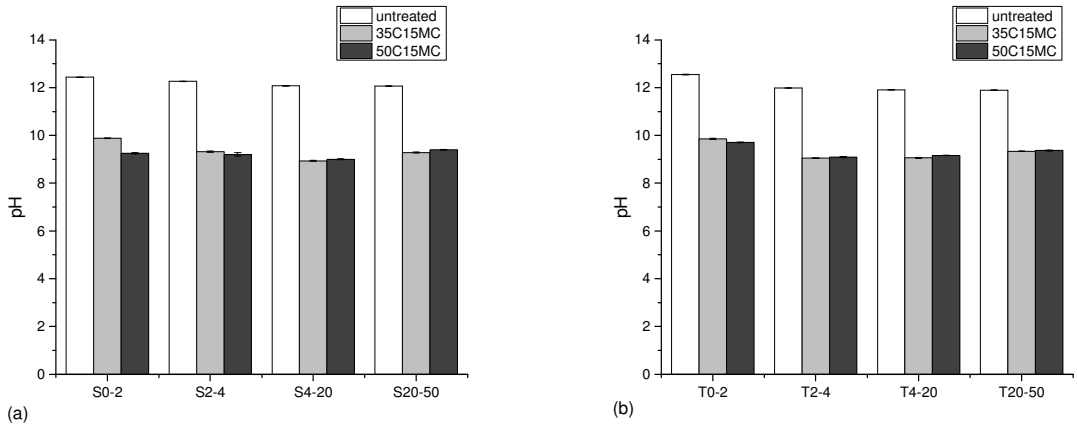

Figure 4. XRD patterns of untreated and carbonated at 50°C and 15% moisture content of (a) T0-2 and (b) T20-50 samples. [An = anhydrite, Ca = calcite, H = hematite, M = magnetite, P = portlandite, Q = quartz]

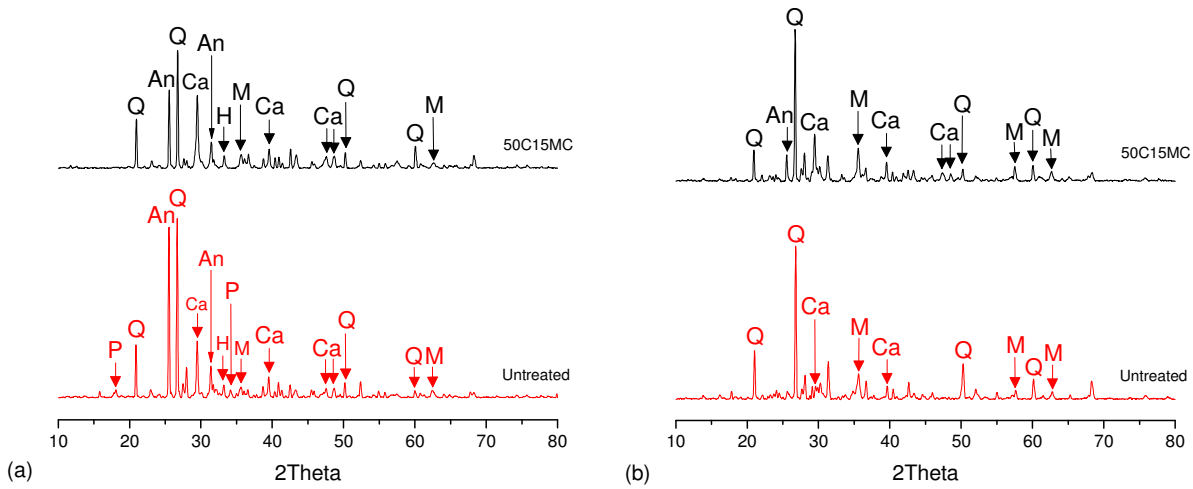

Figure 5. Zn, Cu, and Cr release as a function of size fractions for untreated and carbonated (a, c, e) S and (b, d, f) T samples.

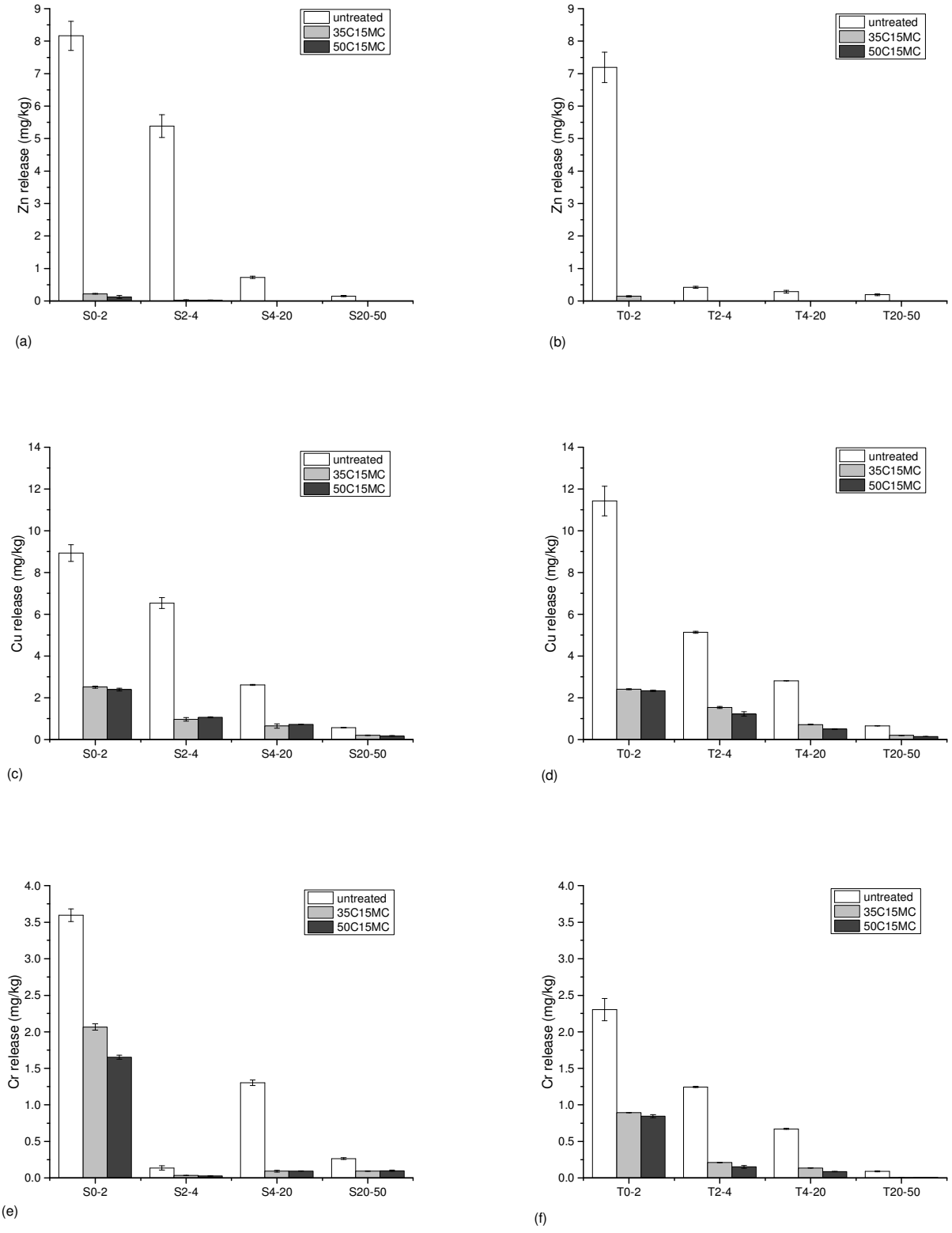

Figure 6. Correlation between Cu and DOC leaching for the different size fractions of S and T samples carbonated for 2 hrs at 15% moisture content and (a, c) 35°C and (b, d) 50°C. R = Pearson's R.

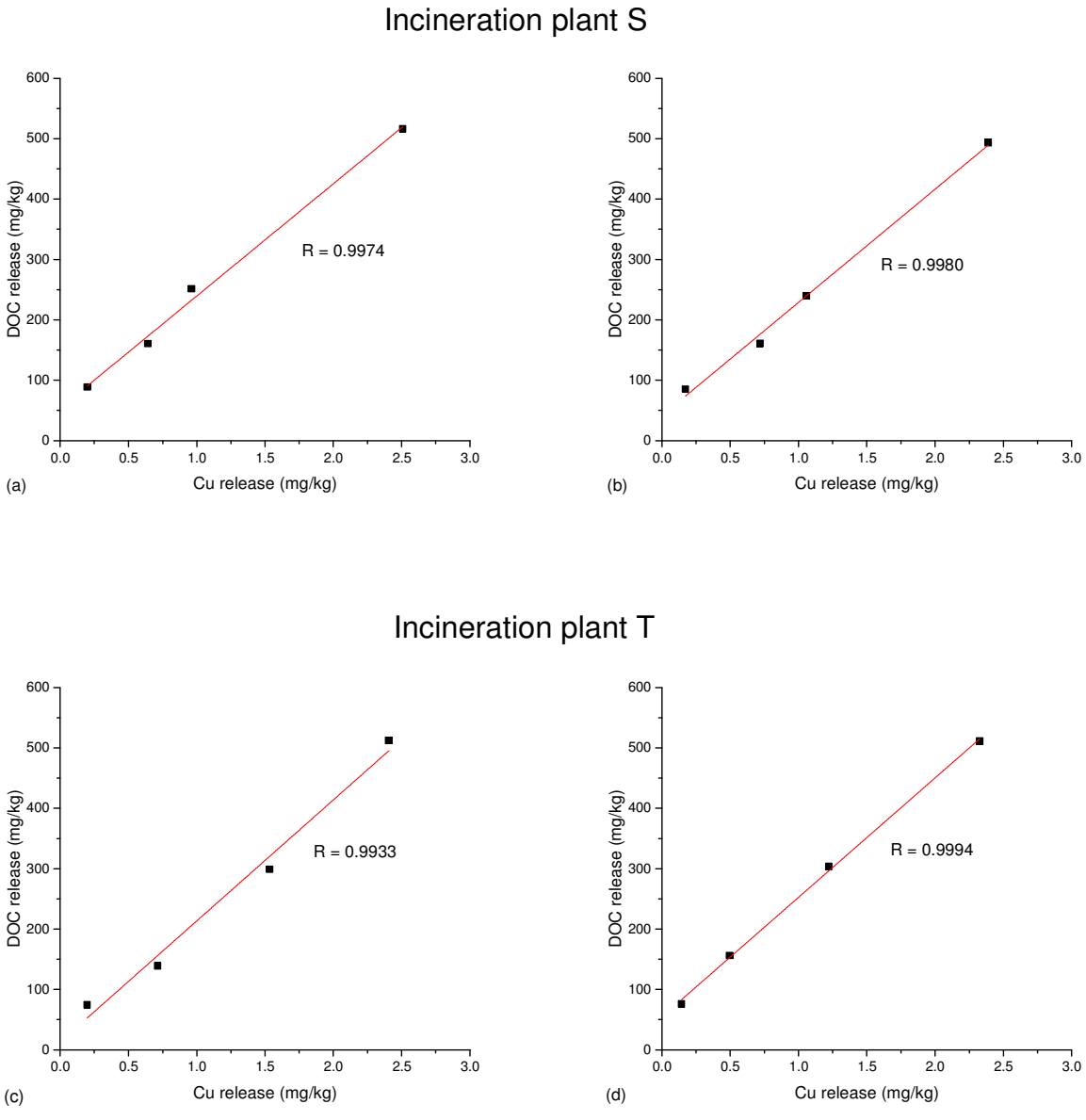

Figure 7. DOC, Cl^- and SO_4^{2-} release as a function of size fractions for untreated and carbonated (a, c, e) S and (b, d, f) T samples.

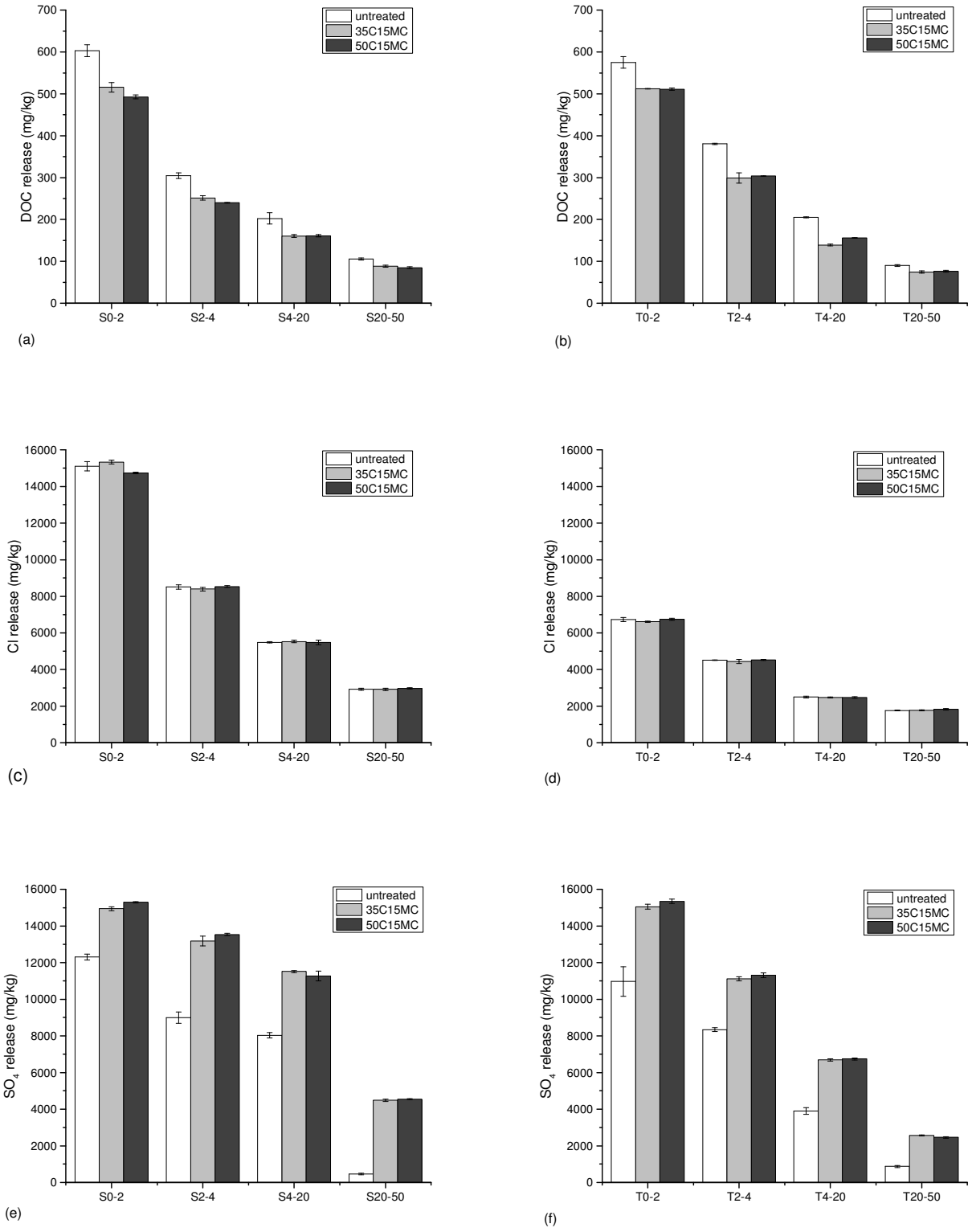

Figure 8. The acid neutralising capacity (ANC) of the different size fractions of untreated (a) S and (b) T samples.

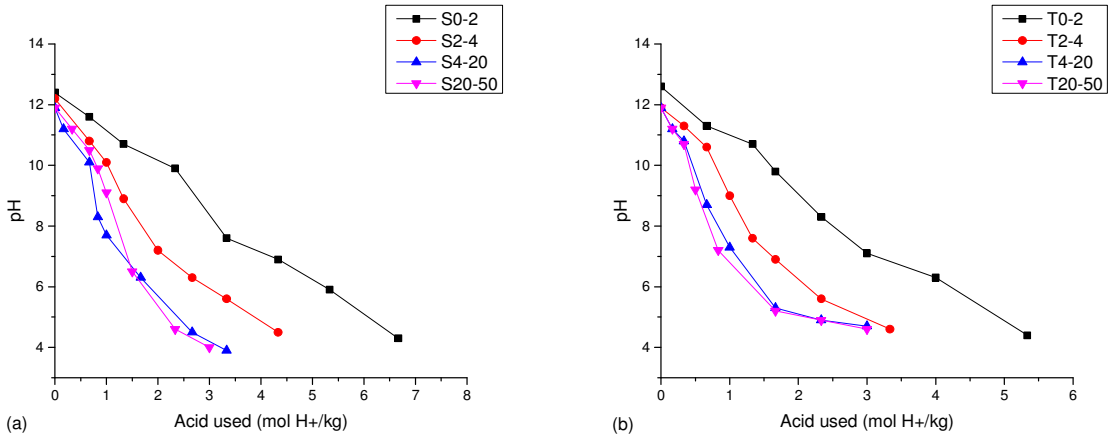

1 **TABLES**

2 Table 1. Characteristics of IBA collected from incineration plant S and T.

Incineration plant	**S**		**T**	
Moisture content (%)	16.8		15.5	
LOI (%)	0.59		1.51	
Ferrous (wt%)	12.1		8.3	
Non-ferrous (wt%)	0.8		1.2	
Size fraction	**0-2 mm**	**2-4 mm**	**4-20 mm**	**20-50 mm**
Particle size distribution (wt%)	34.2 (S) 29.7 (T)	8.6 (S) 7.3 (T)	38.7 (S) 29.9 (T)	14.5 (S) 20.1 (T)
True density (kg/m^3)	2,782 (S) 2,928 (T)	2,822 (S) 2,997 (T)	2,766 (S) 3,023 (T)	2,772 (S) 3,099 (T)

3

4

1 Table 2. Total element content (mg/kg) for the four size fractions of IBA from incineration plants S and T.

Element	S				T			
	0-2 mm	**2-4 mm**	**4-20 mm**	**20-50 mm**	**0-2 mm**	**2-4 mm**	**4-20 mm**	**20-50 mm**
Ag	19	13	9	9	18	19	7	10
Al	32,467	33,767	30,600	62,900	32,033	37,867	36,667	40,167
As	20	24	37	17	64	63	38	24
Ba	81	57	41	52	65	74	66	50
Be	0.9	1.2	1.5	3.4	1.2	1.4	1.7	1.7
Ca	180,333	132,000	108,000	84,067	139,667	108,667	103,267	93,867
Cd	11	2.1	1.4	0.58	5.3	1.8	1.1	< 0.5
Co	52	34	30	17	48	41	33	28
Cr	235	216	184	140	206	210	248	287
Cu	2,453	3,513	1,703	733	2,437	2,070	2,243	1,883
Fe	51,467	59,067	56,700	51,067	111,000	117,333	133,667	141,000
K	9,270	9,447	8,977	14,500	9,857	10,467	9,970	9,363
Mg	10,113	9,723	11,133	8,217	10,633	10,300	11,367	11,433
Mn	895	1,030	679	718	1,600	2,127	1,987	1,733
Mo	17	14	11	8	121	96	85	88
Na	15,333	22,700	41,667	19,033	13,067	17,100	25,967	17,467
Ni	183	140	92	88	169	172	130	107
Pb	611	1,717	1,133	145	199	294	288	122
Sb	246	153	131	84	85	59	57	34
Sn	161	130	99	113	95	94	63	73
Sr	340	388	521	736	327	348	502	252
Ti	6,720	5,297	3,450	3,350	5,267	6,163	5,527	5,817
V	27	30	24	40	55	53	49	65
Zn	3,073	2,387	1,523	1,900	4,050	2,953	2,147	1,437
Cl	11,200	6,493	3,877	1,887	5,900	3,687	1,940	1,290
SO_4	8,307	6,440	4,890	1,880	6,987	5,320	3,143	1,433

2

Table 3. The degree of carbonation (mg/g) of the respective IBA size fractions and the actual moisture content (%) remaining after 2 hours of carbonation. (*35C = 35°C, 50C = 50°C, 15MC = 15% moisture content)

Operating conditions	Degree of carbonation (mg/g)	Actual moisture content (%)
S0-2		
35C15MC	9.20 ± 0.59	14.00
50C15MC	8.79 ± 0.80	9.58
S2-4		
35C15MC	4.34 ± 0.12	15.18
50C15MC	3.78 ± 0.13	11.25
S4-20		
35C15MC	3.55 ± 0.25	14.31
50C15MC	3.26 ± 0.47	11.00
S20-50		
35C15MC	4.42 ± 0.11	14.75
50C15MC	4.47 ± 0.26	10.75
T0-2		
35C15MC	8.56 ± 1.50	13.31
50C15MC	10.41 ± 0.47	12.03
T2-4		
35C15MC	4.89 ± 1.25	14.31
50C15MC	6.53 ± 0.94	10.50
T4-20		
35C15MC	4.15 ± 0.69	14.09
50C15MC	4.11 ± 0.76	9.75
T20-50		
35C15MC	2.51 ± 0.34	14.53
50C15MC	2.86 ± 0.31	9.75